Makara Journal of Science

Volume 26
Issue 3 *September*

Article 2

9-30-2022

Estimation of the Bubble Point Pressure of Multicomponent Reservoir Hydrocarbon Fluids

Benjamin Sunday Usen
Department of Pure and Industrial Chemistry, Faculty of Science, University of Port Harcourt, Choba 5323, Nigeria

Chidi Obi
Department of Pure and Industrial Chemistry, Faculty of Science, University of Port Harcourt, Choba 5323, Nigeria, zarasexcom@yahoo.com

Makara Journal of Science, 26/3 (2022), 151–165
doi: 10.7454/mss.v26i3.1331

Estimation of the Bubble Point Pressure of Multicomponent Reservoir Hydrocarbon Fluids

Benjamin Sunday Usen and Chidi Obi*

Department of Pure and Industrial Chemistry, Faculty of Science, University of Port Harcourt, Choba 5323, Nigeria

*E-mail: chidi.obi@uniport.edu.ng

Received March 15, 2022 | Accepted August 26, 2022

Abstract

This study developed a novel C-sharp (C#) programming language for the estimation of bubble point pressure (BPP) of various hydrocarbon mixtures at equilibrium state. The methodology was based on vapor–liquid equilibrium calculation using Peng Robinson equation of state implementation, thermodynamic equilibrium calculation and Newton-Raphson's method for the successive substitution of the unknown variables. The equal fugacity constraint can be satisfied by obtaining the equilibrium which serves as a criterion for two or more phases to exist at equilibrium. The problem was resolved by searching for a pressure that will satisfy the two constraints. Complex calculation was performed by successively substituting the pressure value estimated by Newton–Raphson's method at reservoir temperature until the two constraints were satisfied. The BPP values for the eight reservoir sample fluids were within the range of 29.32–308.00 atm with an absolute error deviation ranging from 0.00–4.27 and average percentage error of 0.54%. BPP values were obtained were within the reservoir temperature range of 328.15–398.71 K. This procedure is a potential approach for the estimation of BPP for hydrocarbon mixtures with defined fluid composition irrespective of their composition.

Keywords: bubble point pressure, hydrocarbon fluids, equation of state, thermodynamic properties, vapor–liquid equilibrium

Introduction

Petroleum reservoir fluids are composed mainly of hydrocarbon and other related compounds, such as sulphides, nitrogen, and carbon (IV) oxide. Water is also present in gas and oil reservoirs in an interstitial form. The influence of water on the phase behavior and properties of hydrocarbon fluids is of great concern because of the formation of hydrates [1].

The phase behavior of oil and gas is usually modeled without considering water phase except in cases where water–hydrocarbon solids known as hydrates are present. Hydrates are not common and are only present in reservoirs located around the polar axis. When not handled properly, this formation can lead to multiphase flow, flow blockage, and other engineering challenges [2]. The phase behavior of hydrocarbon mixture is majorly dependent on the reservoir pressure, temperature, and fluid chemical composition. This behavior is of a prime consideration in the development and management of reservoirs because it affects all aspects of petroleum exploration and production.

Although a reservoir fluid may be composed of thousands of compounds, the fundamentals of its phase can be explained by examining the behavior of its pure and simple multicomponent mixtures. The behavior of all real reservoir fluids basically follows the same principle and has been classified as the dry gas, wet gas, gas condensate, volatile oil, or black oil [1, 3].

According to Sayani *et al.* [1], accurate and reliable phase behavior and volumetric data are essential elements for the proper management of petroleum reservoirs. This information is required to evaluate reserves, develop the optimum recovery plan, and determine the quantity and quality of produced fluids. Most reservoirs are produced by depletion in which the reservoir pressure declines as fluids are recovered. The reservoir temperature stays practically constant in most recovery methods (isothermal). Therefore, the reservoir pressure is the main variable that determines the behavior of fluids during depletion. Hence, relatively simple tests that simulate recovery are conducted by varying the fluid pressure. The main emphasis is on the bubble point pressure (BPP) in the reservoir and at different surface temperatures.

As an important reservoir fluid property, BPP is the key parameter used in designing the phase diagram of a fluid system [4, 5]. Bubble point curve is one of the boundaries showing the distinction between two phases (liquid and

vapor) and the gaseous phase [1] and is constructed using BPP values obtained at different temperatures [5].

For a pure component, the BPP simply means the pressure at which the first bubble of gas is detected [6, 7]. Given the involvement of the pressure, volume, and temperature (PVT) relationship in BPP, equations of state are applied in estimating BPP and other vapor–liquid equilibrium (VLE) parameters [8].

In thermodynamics, BPP is the pressure (at a given temperature) where the first bubble of vapor is formed when heating a liquid consisting of two or more components [9]. The obtained vapor always has different compositions for each component present in the liquid phase and cannot be identified easily unless it is simplified by assuming the equilibrium state. Reservoir fluids are considered to exist in two phases (liquid and gas) on the basis of reservoir pressure and temperature conditions. When these fluids are recovered, phase separation or phase split is observed. The separation design involves VLE calculations to determine the amount of each component distributed in each phase.

At bubble point, the following relationship holds:

$$\sum_{i=1}^{Nc} y_i = \sum_{i=1}^{Nc} K_i x_i = 1 \quad (1)$$

$$K_i = \frac{y_i}{x_i} \quad (2)$$

where K_i is the distribution coefficient or k-factor, defined as the ratio of mole fraction in the vapor phase (y_i) to the mole fraction in the liquid phase (x_i) at equilibrium.

In the simplest approach of predicting PVT data, the reservoir oil is considered to be composed of two components namely gas and oil. These components are identified by flashing the reservoir fluid at the standard conditions, and characterizing the separated gas and oil phases by their specific gravity and molecular weight values [10].

Several experimental correlations have been developed to estimate this physical property; however, they can only estimate the bubble point for oil compositions whose correlations have been established [11, 12]. In addition, these laboratory experiments are laborious, time consuming, and not totally reproducible. By contrast, computational correlations are economically advantageous and enhance the speed of investigations.

Equation of state (EOS) model is a 1 D approach that satisfies equation 1 in estimating BPP [13]. This semi empirical expression relates pressure (P;) to temperature (T;), and volume (V;). A proper description of this PVT relationship for real hydrocarbon fluids is essential in determining the volumetric and phase behavior of petroleum reservoir fluids and predicting the performance of surface separation facilities. In general, most EOS models require only the fluid composition, critical properties and acentric factor of individual components [14] and to some extent, the boiling temperature and specific gravity for the characterization of heavy fractions. The main advantage of using an EOS is that the same equation can be used to model the behavior of all phases, thereby ensuring consistency when performing phase equilibrium calculations [15].

Numerous EOS models have been developed to correlate the PVT behavior of real fluids with experimental data. For an exact expression of the PVT relationship in real fluids, a correction factor named compressibility factor; (also known as gas deviation factor or simply Z-factor) was introduced to account for the difference of real fluids from ideality. This factor can be expressed as:

$$Z = \frac{V_{real}}{V_{ideal}} \quad (3)$$

The real gas equation is given as:

$$P = \frac{ZRT}{V_{real}} \quad (4)$$

Owing to the extreme limitations of the applicability of equations (3) and (4), numerous attempts have been made to develop an EOS suitable for describing the behavior of real fluids at extended ranges of pressures and temperatures. The two equations above do not apply to the liquid phase; hence they do not capture phase changes in this state. Developments and advancements made in the field of empirical cubic EOS gave rise to van der Waals, Redlich–Kwong, Soave Redlich Kwong (SRK), and Peng–Robinson (PR); the latter two are the two most used EOS in petroleum engineering industries [16].

Peng and Robinson [17] comprehensively evaluated the use of SRK EOS in predicting the behavior of naturally occurring hydrocarbon systems. Their study illustrated the need to improve the ability of EOS in predicting liquid densities and other fluid properties, particularly under critical conditions.

To provide a basis for creating an improved model, Peng and Robinson proposed the following expression:

$$P = \frac{RT}{V-b} - \frac{a\alpha(T)}{V(V+b)+b(V-b)} \quad (5)$$

where

$$a = 0.45724 \frac{R^2 T_C^2}{P_C} \quad (6)$$

$$b = 0.07780 \frac{RT_C}{P_C} \quad (7)$$

$$\alpha = \left[1 + m\left(1 - \sqrt{T_r}\right)^{1/2}\right]^2 \quad (8)$$

If $\omega \leq 0.49$;

$$\text{then } m = 0.37464 + 1.54226\omega - 0.26992\omega^2 \quad (9)$$

If $\omega > 0.49$;

$$\text{then } m_i = 0.379642 + 1.485036\omega - 0.164423\omega^2 + 0.016666\omega^3 \quad (10)$$

Some recently proposed noncubic EOS models, which were derived using thermodynamics, have also been increasingly applied in chemical industries. Compared with cubic EOS, noncubic EOS generally has an in-depth theoretical basis but features mathematical complexities and large computational efforts, whether this extra computational effort translates to significantly improved phase behavior predictions is yet to be evaluated [18]. A work on the comparison of PR cubic EOS and perturbed chain statistical associating fluid theory concluded that the bubble point curves predicted by both EOS are usually similar [18]. Cubic EOS is traditionally used by the oil and gas industries to model phase behavior because they have good results and are mathematically simple [19]. Among which, PR EOS is the most widely used [20].

Considering the unknown value of distribution coefficient at equilibrium, this study applied Wilson's correlation and EOS to check the equal fugacity criteria to obtain the accurate K-values. The problem required solving "4n+1" equations for an n number of components.

Therefore, this study aimed to develop a simplified EOS model using the C-sharp (C#) computational package for the BPP estimation in hydrocarbon mixtures.

Materials and Methods

Materials. C# console application was adopted in computing and testing of the procedure. The procedure was tested using eight reservoir hydrocarbon fluid samples (labeled A–H) containing well-characterized substances, i.e., without lumped heavy fractions such as C_{7+}. The sample data were obtained from CypherCrescent Nigeria Limited, Port Harcourt.

Procedure. BPP was calculated using equation 11:

$$F(n_V) = \sum_i^N \left[\frac{z_i(K_i - 1)}{1 + n_V(K_i - 1)}\right] \quad (11)$$

At the bubble point, the number of moles of the vapor phase, n_v was equal to zero (0). The only phase in existence was liquid showing that the liquid mole fraction (x_i) was equal to the total phase composition (z_i).

$$x_i = z_i \quad (12)$$

Vapor phase composition, y_i, was given as:

$$y_i = K_i z_i \quad (13)$$

Equation (11) was transformed as:

$$\sum_i^N z_i K_i - \sum_i^N z_i = 0 \quad (14)$$

The sum of the phase composition was equal to 1.

$$1 - \sum_i^N z_i K_i = 0 \quad (15)$$

The problem became the search for an equilibrium ratio (K-values) that will satisfy equation (15).

When equation (15) was equated to zero, the problem was reduced to finding a root as equilibrium values for all ith components.

The K-values were not known in advance and were estimated using Wilson's K-value correlation:

$$K_i = \frac{P_{ci}}{P} \exp\left[5.37(1 + \omega_i)\left(1 - \frac{T_{ci}}{T}\right)\right] \quad (16)$$

In the search for the equilibrium ratio, the equal fugacity constraint must be satisfied. This constraint is related to the state of thermodynamic equilibrium as stated in equation (17):

$$f_i^L = f_i^V \quad (17)$$

where f_i^L and f_i^V represent the fugacity of ith component in liquid and vapor phases, respectively.

Hence, equation (17) was solved by setting up PR EOS [17].

However, equation (16) does not satisfy equation (17) at first iteration; hence, substitution was required.

Equation (16) was modified by introducing the concept of fugacity coefficient as stated in equation (18):

$$K_i = \frac{\phi_i^L}{\phi_i^V} \quad (18)$$

Finally, an initial BPP was required to obtain the K-values using Wilson's correlation in equation (16). Most algorithms for BPP estimation using EOS have limitations in determining initial BPP. In this work, the method proposed by Tarek [6] was used by substituting equation (16) into (15).

$$BPP = \sum_i^N z_i P_{ci} \exp\left[5.37(1+\omega_i)\left(1-\frac{T_{ci}}{T}\right)\right] \quad (19)$$

The pressure estimated at the first iteration may not satisfy equations (15) and (17); hence, successive substitution and Newton–Raphson iterative solution for the root problem were applied.

Successive Substitution and Newton Raphson's Iterative Technique. Given the equilibrium ratio is dependent on pressure, equation (12) was expressed as a function of pressure to determine the pressure that can satisfy equations (15) and (16):

$$F(BPP) = 1 - \sum_i^N z_i K_i \quad (20)$$

Substituting equation (18) into (20) and differentiated with respect to BPP gives,

$$F'(BPP) = \sum_i^N \left[z_i K_i \left(\frac{d\phi_i^L}{dBPP} - \frac{d\phi_i^V}{dBPP}\right)\right] \quad (21)$$

Newton–Raphson's numerical method of root finding was applied to update the pressure as follows:

$$P_{j+1} = P_j - \frac{F(BPP)}{F\prime(BPP)} \quad (22)$$

where j represents the current iterate

Error Value and Tolerance. Error value was introduced to check, if the pressure estimated by equation (22) satisfies equations (15) and (17). The error value was calculated either by obtaining the absolute value of equation (20) or using equation (23):

$$\text{Error value} = |P_{j+1} - P_j| \quad (23)$$

As a numerical procedure, equation (20) was not expected to be equal to zero in accordance with its theoretical definition. Hence, a numerically approximated value referred to as tolerance was used. In this work, tolerance was set to 1 x 10^{-12}.

Binary Interaction Parameters (BIPs), which were obtained with the sample data from cypherCrescent, were used to improve the predictive capability of PR EOS.

PR EOS Model. PR [17] cubic EOS was set up to calculate the compressibility (z-factor) factor of the liquid and incipient vapor phases.

$$P = \frac{RT}{V-b} - \frac{a\alpha(T)}{V(V+b)+b(V-b)} \quad (24)$$

The molar volume was expressed from ideal gas equation as:

Programming Flowchart.

$$\bar{V} = \frac{ZRT}{P} \quad (25)$$

Substituting equation (25) into (24) gives,

$$Z^3 - (1-B)Z^2 + (A - 2B - 3B^2)Z - (AB - B^2 - B^3) = 0 \quad (26)$$

Applying the mixing and combining rule yielded.

$$A = \frac{a_{mix}P}{(RT)^2} \quad (27)$$

and

$$B = \frac{b_{mix}P}{RT} \quad (28)$$

where a_{mix} and b_{mix} are the attractive and repulsive parameters of the mixture, respectively, and were calculated as follows:

$$a_{mix} = \sum_i^{Nc}\left[z_i z_j (a_i a_j)^{1/2}(1-k_{ij})\right] \quad (29)$$

and

$$b_{mix} = \sum_i^{Nc}[z_i b_i] \quad (30)$$

$$a_i = 0.45724\frac{\alpha_i R^2 T_C^2}{P_{ci}} \quad (31)$$

$$b_i = 0.07780\frac{RT_{ci}}{P_{ci}} \quad (32)$$

where z_i, z_j, a_i and a_j represent the phase compositions and attractive parameters of ith and jth components respectively; b_i represents the repulsive parameter of ith component and is dependent on the phase in consideration; k_{ij} represents the binary interaction parameter of components i and j; and N_c is the number of components.

$$\alpha_i = \left[1 + m_i\left(1 - \sqrt{T_{ri}}\right)^{1/2}\right]^2 \quad (33)$$

For $\omega \leq 0.49$,

$$m_i = 0.37464 + 1.54226\omega_i - 0.26992{\omega_i}^2 \quad (34)$$

For $\omega > 0.49$, the modification proposed by Peng and Robinson (1978) was used:

$$m_i = 0.379642 + 1.485036\omega_i - 0.164423{\omega_i}^2 + 0.016666{\omega_i}^3 \quad (35)$$

$$T_{ri} = \frac{T}{T_{ci}} \quad (36)$$

where T_r represents the reduced temperature.

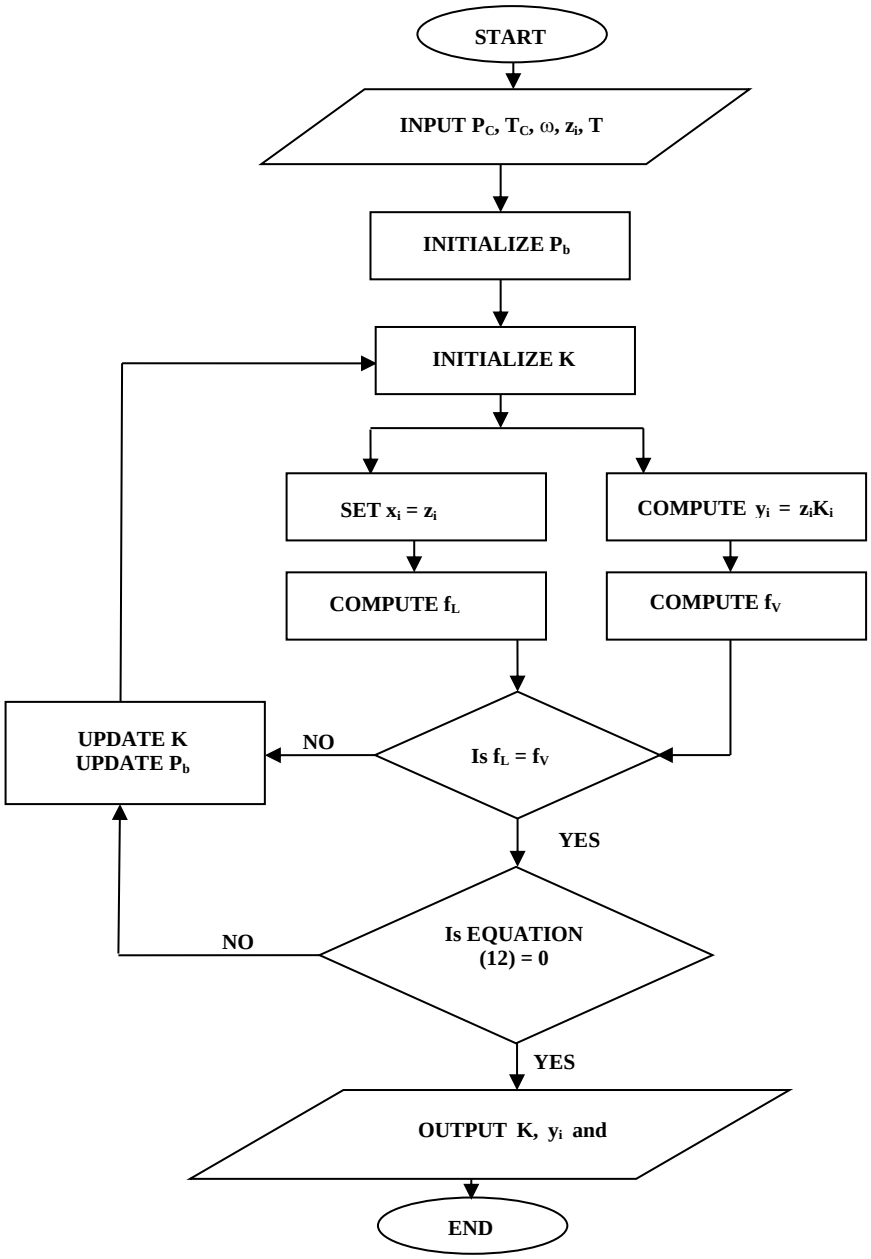

Figure 1. Computation of Bubble Point Pressure (BPP) using EOS

Equation (26) was solved using analytical and numerical (Newton–Raphson's) methods for cubic equations to enhance accuracy at the point where any of the methods failed. In this study, a procedure was written using Newton–Raphson's numerical method for the determination of the root of equations.

Selection Scheme for Cubic Compressibility Factor. Gibbs energy change was calculated using equation (37):

$$\frac{G_h - G_l}{RT} = (Z_h - Z_l) + \ln\left(\frac{Z_l - B}{Z_h - B}\right) - \frac{A}{B(\delta_2 - \delta_1)} \ln\left[\left(\frac{Z_l + \delta_1 B}{Z_l + \delta_2 B}\right)\left(\frac{Z_h + \delta_2 B}{Z_h + \delta_2 B}\right)\right] \quad (37)$$

where $\delta_1 = 1 + \sqrt{2}$ and $\delta_1 = 1 - \sqrt{2}$, Z_h and Z_l represent the highest and lowest root, respectively; G_h and G_l represent the highest and lowest Gibbs energy, respectively; R represents the universal gas constant, and T represents the absolute temperature.

Calculation of Fugacity Coefficient and Fugacity. The fugacity coefficient and fugacity for liquid and vapor phases were calculated using PR EOS with the following expressions:

$$\phi_i^L = \exp\left[\frac{b_i}{b_{mix}}(Z^L - 1) + \ln(Z^L - B) - \frac{A}{2\sqrt{2}B}\left(\frac{2\psi_i^L}{a_{mix}} - \frac{b_i}{b_{mix}}\right)\ln\left(\frac{Z^L + (1+\sqrt{2})B}{Z^L + (1-\sqrt{2})B}\right)\right] \quad (38)$$

$$\phi_i^V = \exp\left[\frac{b_i}{b_{mix}}(Z^V - 1) + \ln(Z^V - B) - \frac{A}{2\sqrt{2}B}\left(\frac{2\psi_i^V}{a_{mix}} - \frac{b_i}{b_{mix}}\right)\ln\left(\frac{Z^V + (1+\sqrt{2})B}{Z^V + (1-\sqrt{2})B}\right)\right] \quad (39)$$

$$f_i^L = x_i\phi_i^L P \quad (40)$$

$$f_i^V = y_i\phi_i^V P \quad (41)$$

where ψ_i for each component in liquid and vapor phase was computed as:

$$\psi_i^L = x_i\sqrt{a_i a_j}(1 - k_{ij}) \quad (42)$$

and

$$\psi_i^V = y_i\sqrt{a_i a_j}(1 - k_{ij}) \quad (43)$$

Results and Discussions

Sample Compositions. The overall composition of the eight reservoir samples is presented in Table 1.

Figure 2 reveals the reservoir temperature of fluid samples. The result showed that hydrocarbon component D had the highest reservoir temperature of 398.706 K.

The Newton–Raphson's iterative numerical mathematical technique coupled with EOS and thermodynamic equilibrium model was applied in BPP estimation for hydrocarbon mixtures and separation facilities [21].

With this method, the pressure in question became the x-value and the pressure at which the BPP function equals or approaches zero (f(BPP) = 0) was the unknown. The bubble point function was dependent on equilibrium ratio. In addition, the equilibrium ratio was not known in advance because the equilibrium ratio, K describes the ratio of the incipient vapor phase composition to the ratio of the liquid phase composition (known phase composition).

Table 1. Sample Compositions in Mole Percentage

Components	A	B	C	D	E	F	G	H
N_2	0.45	0.3	0.16	0.51	1.64	1.28041	0.02	0.15
CO_2	0.44	0.9	0.91	1.19	0.08	1.39161	0.22	-
C_1	35.05	53.47	36.47	45.21	28.4	56.3483	39.86	12.47
C_2	4.64	11.46	9.67	7.09	7.16	7.08725	2.23	0.52
C_3	2.46	8.79	6.95	4.61	10.48	5.09174	2.29	0.29
iC_4	-	-	1.44	1.69	-	1.64371	1.07	0.25
nC_4	1.66	4.56	3.93	2.81	8.4	3.75682	1.69	0.35
iC_5	-	-	1.44	1.55	0	2.08001	1.07	0.42
nC_5	1.6	2.09	1.41	2.01	3.82	2.48871	1.41	0.37
C_6	5.46	1.51	4.33	4.42	4.05	3.65102	2.11	5.34
PS_1	25.1437	4.49495	11.4544	11.1963	13.9994	15.1804	48.03	8.94753
PS_2	23.0963	2.66302	8.90088	4.92885	7.33951	-	-	11.0527
PS_3	-	3.06816	12.9347	4.69996	14.6311	-	-	7.045
PS_4	-	2.82766	-	8.08487	-	-	-	7.97575
PS_5	-	3.86621	-	-	-	-	-	8.79712
PS_6	-	-	-	-	-	-	-	8.20244
PS_7	-	-	-	-	-	-	-	7.31189
PS_8	-	-	-	-	-	-	-	6.28286
PS_9	-	-	-	-	-	-	-	5.23593
PS_{10}	-	-	-	-	-	-	-	8.98881

(Note: PS represents the pseudo split components)

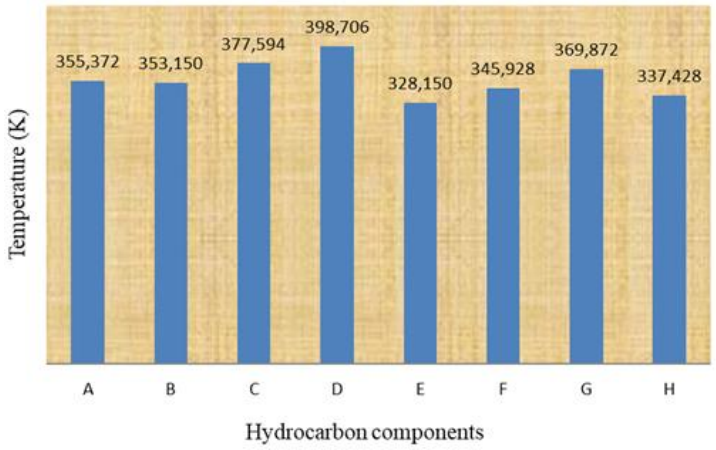

Figure 2. Reservoir Temperatures (in K) of Each Fluid Sample

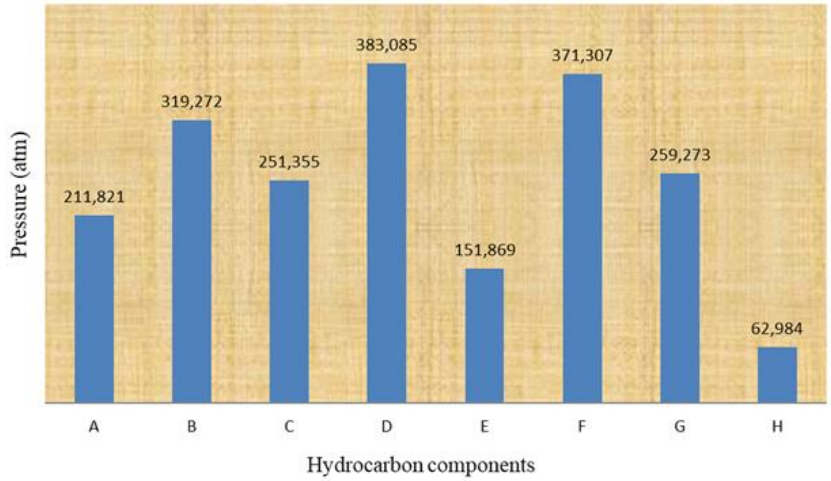

Figure 3. Estimated Pressure in Atmosphere (atm)

The incipient vapor phase composition can only be determined at BPP in question. Hence, successive substitution with a check in BPP function was used. The introduction of this technique led to the estimation of the unknown parameters in BPP function and continuous resubstitution until the BPP function was satisfied. The first estimated parameter was the pressure at which the bubble point function tends to be zero as presented in Figure 3.

This equation satisfactorily estimated pressures that were higher than the expected BPP and can be compared with the initial pressures used in the constant composition experiment.

In constant composition experiment, the starting pressure was always above the BPP and decreased in small steps; the changes available in the system were monitored until the incipient vapor phase was formed [22, 23].

The equilibrium ratio can now be initialized as a function of the estimated pressure and reservoir or separation facility temperature using Wilson's correlation, and the results are presented in Table 2.

The unknown incipient vapor phase composition can now be estimated as the product of equilibrium ratio and liquid phase composition as presented in Table 3.

At the BPP, the summation of the incipient vapor phase composition is expected to be equal to or approximately equal to one [1]. One has to be careful at this point because the summation of the incipient vapor phase composition may be true but at the wrong pressure due to the wrong values of equilibrium ratio; hence, this point was termed as a critical condition [4, 24, 25].

Offsetting this error facilitates the check of thermodynamic equilibrium condition as one of the criteria to ascertain that the BPP was accurately estimated.

Table 2. Initial Equilibrium Ratio Estimated with Wilson's Correlation

Components	A	B	C	D	E	F	G	H
N_2	5.8093	1.4308	3.4902	2.1967	4.6441	1.2409	3.392	17.3674
CO_2	0.903	0.9453	1.499	1.106	1.0464	0.9727	1.0437	-
C_1	2.6823	1.2931	2.0429	1.7083	2.7413	1.1365	2.3492	7.65722
C_2	0.5244	0.9833	1.1697	1.0434	0.9122	0.9569	0.9724	2.08587
C_3	0.1547	0.8503	0.7705	0.7745	0.4615	0.8623	0.5857	0.79778
iC_4	-	-	0.5885	0.6367	-	0.8065	0.4205	0.39995
nC_4	0.0502	0.7444	0.5116	0.5775	0.236	0.7782	0.3553	0.30808
iC_5	-	-	0.3872	0.4699	-	0.7257	0.251	0.1494
nC_5	0.0182	0.6549	0.353	0.4411	0.1263	0.7083	0.2244	0.12432
C_6	0.0071	0.5718	0.247	0.341	0.0687	0.6463	0.1444	0.05089
PS_1	0.0003	0.4224	0.118	0.204	0.0216	0.4615	0.0128	0.00056
PS_2	1E–07	0.3954	0.0636	0.1539	0.0046	-	-	9.8E–06
PS_3	-	0.3589	0.0003	0.0894	2E–06	-	-	1.6E–06
PS_4	-	0.2749	-	0.0096	-	-	-	4.7E–07
PS_5	-	0.0981	-	-	-	-	-	1.1E–07
PS_6	-	-	-	-	-	-	-	4.9E–08
PS_7	-	-	-	-	-	-	-	1.3E–08
PS_8	-	-	-	-	-	-	-	5.7E–09
PS_9	-	-	-	-	-	-	-	2.2E–09
PS_{10}	-	-	-	-	-	-	-	5.2E–07

Table 3. Initial Incipient Vapor Phase Composition

Components	A	B	C	D	E	F	G	H
N_2	0.0261	0.0114	0.0082	0.0203	0.1129	0.0479	0.001	0.02639
CO_2	0.004	0.0052	0.009	0.011	0.0006	0.0069	0.002	-
C_1	0.9402	0.9343	0.9117	0.9199	0.835	0.9224	0.979	0.96366
C_2	0.0243	0.0386	0.0536	0.0356	0.0344	0.0183	0.0117	0.00701
C_3	0.0038	0.0087	0.0123	0.0079	0.0133	0.0032	0.0037	0.00107
iC_4	-	-	0.0012	0.0014	-	0.0004	0.0008	0.00038
nC_4	0.0008	0.0014	0.0024	0.0018	0.0031	0.0007	0.0009	0.00039
iC_5	-	-	0.0004	0.0005	-	0.0001	0.0003	0.0002
nC_5	0.0003	0.0002	0.0003	0.0005	0.0005	0.0001	0.0003	0.00014
C_6	0.0004	7E–05	0.0004	0.0005	0.0002	8E–05	0.0002	0.00075
PS_1	8E–05	5E–05	0.0003	0.0004	0.0001	1E–05	8E–05	1.3E–05
PS_2	3E–08	2E–05	5E–05	7E–05	6E–06	-	-	4.4E–07
PS_3	-	1E–05	3E–09	2E–05	4E–10	-	-	6.1E–08
PS_4	-	2E–06	-	9E–08	-	-	-	2.6E–08
PS_5	-	4E–09	-	-	-	-	-	9.7E–09
PS_6	-	-	-	-	-	-	-	4.7E–09
PS_7	-	-	-	-	-	-	-	1.5E–09
PS_8	-	-	-	-	-	-	-	7.1E–10
PS_9	-	-	-	-	-	-	-	2.9E–10
PS_{10}	-	-	-	-	-	-	-	3.7E–09
Total	1	1	1	1	1	1	1	1

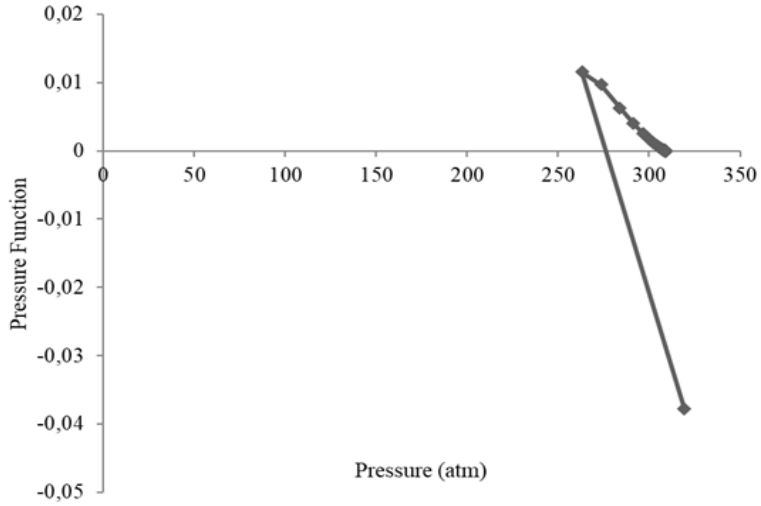

Figure 4. Pressure Function Against Pressure for Sample B

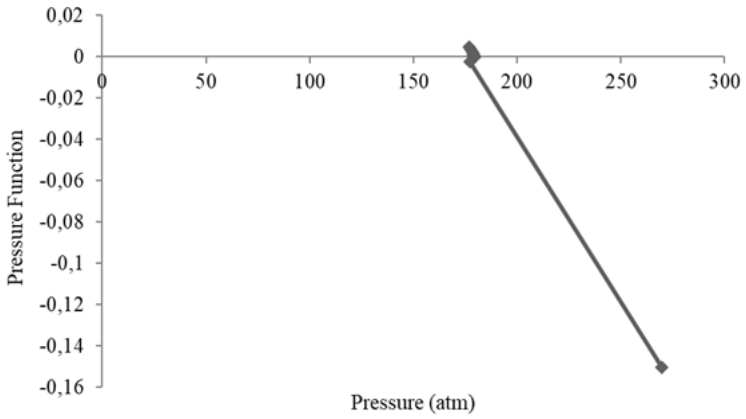

Figure 5. Pressure Function Against Pressure for Sample C

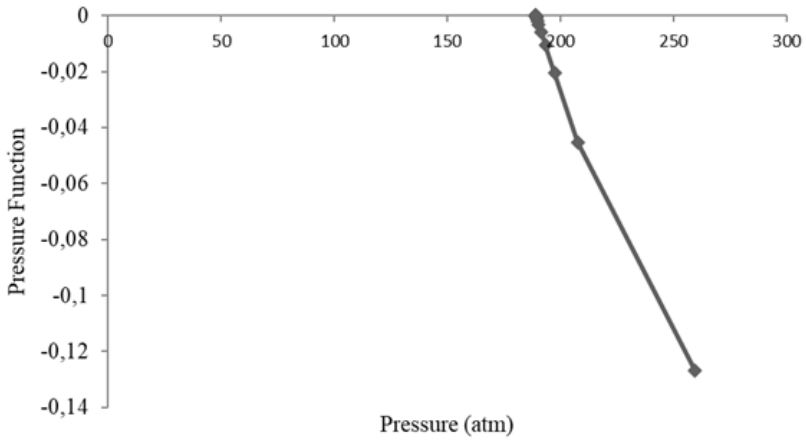

Figure 6. Pressure Function Against Pressure for Sample G

Despite its limitations, modified PR [14] EOS plays a vital role in the calculation of the compressibility factor of the vapor and liquid phases when coupled with numerical and analytical methods for solving cubic equation [26]. In this study, this method was improved by introducing BIPs; a scheme for selecting the correct root that best represents the compressibility factor by checking the root with the least Gibbs free energy [27].

The equilibrium ratio was substituted from the ratio of the fugacity of liquid to the ratio of fugacity of incipient vapor phase until the equal fugacity constraint was satisfied.

For the validation of the proposed method, Figures 4–6 typically illustrate the variation of pressure with respect to iterative estimated pressure, P for fluid samples (B, C, and G). The high initial pressure value gave a negative value of pressure function. A rapid increase in pressure function was then observed at the second iteration, followed by a slight change in the iterated pressure that led the point of convergence where BPP was established. At this point, the pressure function tended to be zero. Though; the number of iterations was large, the use of computer program eased the application of this method compared with the use of Microsoft Excel spreadsheet.

BPP. The results of the comparison among EOS, calculated BPP, and experimental data for all the hydrocarbon components are presented in Table 4 and Figure 7. The error deviations in Table 4 between the calculated and experimental BPPs ranged from 0% to 1.6% with an average error deviation of 0.54%.

The results from this study were compared with those obtained by Coat and Smart [28], Whitson and Brule [29], Ahmed and Nathan [27], Soreide [30] and Ukwu [31].

The present results were found to be better than the existing result, except for that reported by Ukwu [31] offering a better finding for only sample B. The proposed procedure proffered an excellent match for samples A, C, F and G and deviations of 4.273, 3.522 and 1.523 for samples B, D, and, E respectively. The large deviations observed with samples B, D and E may be attributed to the presence of volatile oil of which 80.75% or more of its volume appeared in the vapor phase at stock tank condition [32].

Table 4. Comparison of Experimental and Predicted Bubble Point

S/N	Sample	Temp (K)	Bubble Point Pressure (BPP) (atm)							Error Analysis	
			Expt.	Coat and Smart [28]	Soreide [30]	Whitson and Brule [29]	Ahmed and Nathan [27]	Ukwu [31]	Current Study	Absolute	%
1	A	355.37	172.48		167.19		170.18	172.29	172.48	0.00	0.00
2	B	353.15	304.51	227.55	268.71		306.34	304.16	308.78	4.27	1.40
3	C	377.59	179.30			177.59			179.28	0.02	0.01
4	D	398.71	221.19						224.72	3.52	1.59
5	E	328.15	116.29	104.18	113.09		106.97	115.88	117.81	1.52	1.31
6	F	345.93	259.19						259.19	0.00	0.00
7	G	369.87	189.03						189.03	0.00	0.00
8	H	337.43	29.31						29.32	0.01	0.03
Average Percentage error											0.54

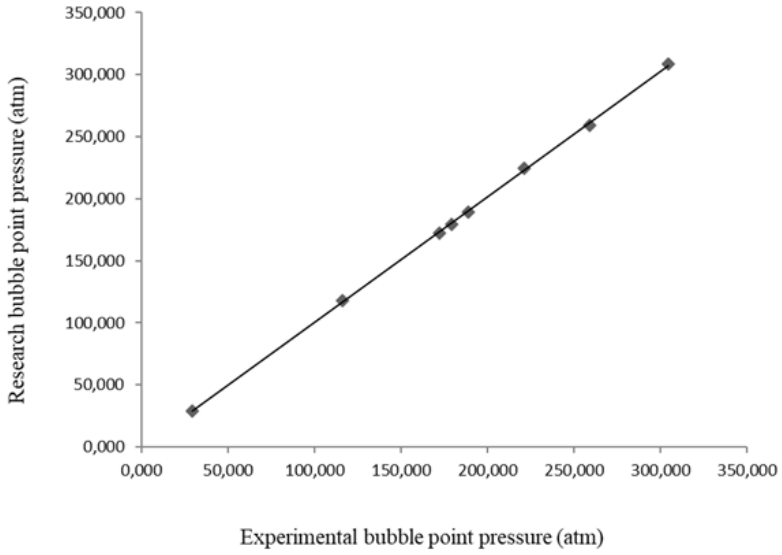

Figure 7. Plot of Experimental Bubble Point Pressure (BPP) Against Calculated Pressure

Table 5. Equilibrium Ratio at Bubble Point Pressure (BPP)

Components	A	B	C	D	E	F	G	H
N_2	5.8093	1.4308	3.4902	2.1967	4.6441	1.2409	3.392	17.3674
CO_2	0.903	0.9453	1.499	1.106	1.0464	0.9727	1.0437	-
C_1	2.6823	1.2931	2.0429	1.7083	2.7413	1.1365	2.3492	7.65722
C_2	0.5244	0.9833	1.1697	1.0434	0.9122	0.9569	0.9724	2.08587
C_3	0.1547	0.8503	0.7705	0.7745	0.4615	0.8623	0.5857	0.79778
iC_4	-	-	0.5885	0.6367	-	0.8065	0.4205	0.39995
nC_4	0.0502	0.7444	0.5116	0.5775	0.236	0.7782	0.3553	0.30808
iC_5	-	-	0.3872	0.4699	-	0.7257	0.251	0.1494
nC_5	0.0182	0.6549	0.353	0.4411	0.1263	0.7083	0.2244	0.12432
C_6	0.0071	0.5718	0.247	0.341	0.0687	0.6463	0.1444	0.05089
PS_1	0.0003	0.4224	0.118	0.204	0.0216	0.4615	0.0128	0.00056
PS_2	1E–07	0.3954	0.0636	0.1539	0.0046	-	-	9.8E–06
PS_3	-	0.3589	0.0003	0.0894	2E–06	-	-	1.6E–06
PS_4	-	0.2749	-	0.0096	-	-	-	4.7E–07
PS_5	-	0.0981	-	-	-	-	-	1.1E–07
PS_6	-	-	-	-	-	-	-	4.9E–08
PS_7	-	-	-	-	-	-	-	1.3E–08
PS_8	-	-	-	-	-	-	-	5.7E–09
PS_9	-	-	-	-	-	-	-	2.2E–09
PS_{10}	-	-	-	-	-	-	-	5.2E–07

The absolute error was obtained by calculating the absolute value of the difference between the experimental and calculated BPPs, and the percentage error was calculated by multiplying the absolute error by 100.

Equilibrium Ratio (K) at BPP. The equilibrium ratios that satisfy equation (15) are presented in Table 5.

The equilibrium ratio confirmed the existence of vapor at equilibrium with the liquid phase proving that the BPP can be estimated not only at any pressure of the liquid at reservoir temperature but also at any pressure at which a minute amount of vapor was present. The equilibrium ratio estimated by Wilsons's correlation may satisfy equation (15) but may not satisfy thermodynamic equilibrium condition (equal fugacity constraint). This defect can be corrected iteratively using the EOS model by substituting the equilibrium ratio from the ratio of the fugacity coefficient of liquid phase (known) composition to the ratio of the incipient vapor phase composition of each component.

Vapor Phase Composition (y) at BPP. The incipient vapor phase compositions at BPP are presented in Table 6.

According to Whitson, if the estimated pressure at a given temperature is the BPP, then the sum of the vapor phase composition must be equal to unity at BPP [32].

The vapor phase composition was dependent on the accurate values of the equilibrium ratio as computed using equation (13).

Evaluation of Fugacity at BPP. Tables 7a and 7b show that the obtained fugacity was equal to for both phases, thus satisfying the criteria for thermodynamic equilibrium.

Evaluation of Gibbs Free Energy. According to Table 8, the Gibbs free energy at BPP was not the same in both phases because their compositions were different. Hence, the criterion for equilibrium was that the change in Gibbs free energy, dG must be less than zero at constant temperature and pressure [6].

Table 6. Vapor Phase Composition at Bubble Point Pressure (BPP)

Samples	A	B	C	D	E	F	G	H
N_2	0.0224	0.0043	0.0056	0.0112	0.0762	0.0189	0.0007	0.0261
CO_2	0.0066	0.0085	0.0136	0.0132	0.0008	0.0152	0.0023	-
C_1	0.8855	0.6914	0.7451	0.7723	0.7785	0.7417	0.9364	0.9549
C_2	0.0506	0.1127	0.1131	0.074	0.0653	0.0671	0.0217	0.0108
C_3	0.015	0.0747	0.0535	0.0357	0.0484	0.0369	0.0134	0.0023
iC_4	-	-	0.0085	0.0108	-	0.0099	0.0045	0.001
nC_4	0.0057	0.0339	0.0201	0.0162	0.0198	0.0222	0.006	0.0011
iC_5	-	-	0.0056	0.0073	-	0.0108	0.0027	0.0006
nC_5	0.0033	0.0137	0.005	0.0089	0.0048	0.0125	0.0032	0.0005
C_6	0.0068	0.0086	0.0107	0.0151	0.0028	0.0165	0.003	0.0027
PS_1	0.0041	0.019	0.0135	0.0228	0.003	0.0483	0.0062	5E – 05
PS_2	2E – 05	0.0105	0.0057	0.0076	0.0003	-	-	1E – 06
PS_3	-	0.011	4E – 05	0.0042	2E – 07	-	-	1E – 07
PS_4	-	0.0078	-	0.0008	-	-	-	4E – 08
PS_5	-	0.0038	-	-	-	-	-	1E – 08
PS_6	-	-	-	-	-	-	-	4E – 09
PS_7	-	-	-	-	-	-	-	9E – 10
PS_8	-	-	-	-	-	-	-	4E – 10
PS_9	-	-	-	-	-	-	-	1E – 10
PS_{10}	-	-	-	-	-	-	-	5E – 08

Table 7a. Fugacity of Liquid and Vapor Phases at Bubble Point Pressure (BPP)

Components	A		B		C		D	
	f_V	f_L	f_V	f_L	f_V	f_L	f_V	f_L
N_2	65.56	65.56	32.25	32.25	19.14	19.14	49.28	49.28
CO_2	11.96	11.96	21.67	21.67	27.22	27.22	32.80	32.80
C_1	1951.52	1951.52	2911.57	2911.57	1832.24	1832.24	2440.65	2440.65
C_2	71.24	71.24	189.41	189.41	168.59	168.59	141.22	141.22
C_3	15.07	15.07	67.70	67.70	54.42	54.42	47.11	47.11
iC_4	-	-	-	-	6.48	6.48	10.85	10.85
nC_4	4.13	4.13	16.41	16.41	14.03	14.03	14.90	14.90
iC_5	-	-	-	-	2.89	2.89	5.06	5.06
nC_5	1.73	1.73	3.77	3.77	2.43	2.43	5.80	5.80
C_6	2.62	2.62	1.48	1.48	3.70	3.70	7.12	7.12
PS_1	0.56	0.56	1.34	1.34	2.48	2.48	6.71	6.71
PS_2	7.16E – 05	7.16E – 05	0.55	0.55	0.54	0.54	1.55	1.55
PS_3	-	-	0.37	0.37	1.45E – 05	1.45E – 05	0.42	0.42
PS_4	-	-	0.08	0.08	-	-	3.63E – 03	3.63E – 03
PS_5	-	-	2.69E – 04	2.69E – 04	-	-	-	-

Table 7b. Continuation of Fugacity of Liquid and Vapor Phases at Bubble Point Pressure (BPP)

Components	E		F		G		H	
	f_V	f_L	f_V	f_L	f_V	f_L	f_V	f_L
N_2	149.84	149.84	113.79	113.79	2.19	2.19	11.36	11.36
CO_2	1.03	1.03	32.26	32.26	4.67	4.67	-	-
C_1	1166.81	1166.81	2558.95	2558.95	2304.15	2304.15	397.03	397.03
C_2	61.90	61.90	95.35	95.35	34.94	34.94	4.11	4.11
C_3	32.10	32.10	27.68	27.68	15.75	15.75	0.82	0.82
iC_4	-	-	4.71	4.71	4.19	4.19	0.33	0.33
nC_4	9.25	9.25	8.93	8.93	5.18	5.18	0.35	0.35
iC_5	-	-	2.71	2.71	1.82	1.82	0.19	0.19
nC_5	1.60	1.60	2.80	2.80	2.04	2.04	0.14	0.14
C_6	0.66	0.66	2.08	2.08	1.48	1.48	0.78	0.78
PS_1	0.46	0.46	0.89	0.89	0.93	0.93	0.01	0.01
PS_2	0.02	0.02	-	-	-	-	1.49E–04	1.49E–04
PS_3	1.32E–07	1.32E–07	-	-	-	-	1.28E–05	1.28E–05
PS_4	-	-	-	-	-	-	3.92E–06	3.92E–06
PS_5	-	-	-	-	-	-	9.37E–07	9.37E–07
PS_6	-	-	-	-	-	-	3.43E–07	3.43E–07
PS_7	-	-	-	-	-	-	6.97E–08	6.97E–08
PS_8	-	-	-	-	-	-	2.53E–08	2.53E–08
PS_9	-	-	-	-	-		7.41E–09	7.41E–09
PS_{10}	-	-	-	-	-	-	2.77E–06	2.77E–06

Table 8. Gibbs Free Energy at Bubble Point Pressure (BPP)

Sample	G_L	G_V	dG
A	0.678	7.082	−6.404
B	5.003	6.509	−1.506
C	2.364	6.549	−4.185
D	4.112	6.776	−2.664
E	0.221	6.353	−6.132
F	5.823	6.479	−0.656
G	3.257	7.381	−4.124
H	-9.330	5.781	−15.111

(Noted: G_L and G_V represent the Gibbs free energy in the liquid and gas phases, respectively, and dG represents the differential change in Gibbs free energy)

Conclusions

This study demonstrates that the complexity of initial pressure estimation can be reduced by expressing Wilson's correlation in terms of pressure. The following findings were obtained: (a) The BPP for the eight reservoir sample fluids was within the range of 29.315–308.000 atm with absolute deviation ranging from 0.000–4.273 and average percentage error of 0.54%. (b) The reservoir temperatures at which the BPPs were obtained were within the range of 328.150–398.706 K. (c) The equilibrium ratios of each component were all the vectors of positive integers. (d) The Gibbs free energy for the two phases were not the same; hence, the changes in Gibbs free energy were all negative. (e) The fugacity of liquid and vapor phases was all the vectors of positive integers.

Conflict of Interest

The authors declare no conflict of interest.

Acknowledgments

The authors are deeply grateful to CypherCrescent Nigeria Limited, Port Harcourt for providing the raw data.

References

[1] Sayani, J.K.S., Pedapati, S.R., Lal, B. 2020. Phase Behavior Study on Gas Hydrates Formation in Gas Dominant Multiphase Pipelines with Crude Oil and High CO_2 Mixed Gas. Sci. Rep. 10: 14748, https://doi.org/10.1038/s41598-020-71509-6.

[2] Scanlon, B.R., Ikonnikova, S., Yang, Q., Reedy, R.C. 2020. Will Water Issues Constrain Oil and Gas Production in the United States? Environ. Sci. Technol. 54(6): 3510−3519, https://doi.org/ 10.1021/acs.est.9b06390.

[3] Satter, A., Iqbal, G.M. 2016. 4 - Reservoir Fluid Properties. Reserv. Eng. 81−105, https://doi.org/10.1016/B978-0-12-800219-3.00004-8.

[4] El-Banbi, A., Alzahabi, A., El-MaraghiL, A. 2018. Chapter 7 - Black Oils. PVT Property Correlations. In El-Banbi, A., Alzahabi, A., El-MaraghiL, A. (eds.), PVT Property Correlations. Gulf Professional Publishing. English. pp. 147−182, https://doi.org/ 10.1016/B978-0-12-812572-4.00007-2.

[5] Britto, A.F., Lima, I.C.d.C., Lima, A.T.d.C. 2021. Influence of Bubble Point Pressure on the Gas Formation in an Oil Reservoir Under Water Injection. Am. J. Chem. Eng. 9(4): 101−111, https://doi.org/10.11648/j.ajche.20210904.14.

[6] Ahmed, T. 2019. Chapter 15 - Vapor-Liquid Phase Equilibria. In Ahmed, T. (eds.), Reservoir Engineering Handbook, 5th ed. Gulf Professional Publishing. English. pp. 1109−1225.

[7] Alakbari, F.S., Mohyaldinn, M.E., Ayoub, M.A., Muhsan, A.S., Hussein, I.A. 2022. An Accurate Reservoir's Bubble Point Pressure Correlation. ACS Omega. 7(15): 13196−13209, https://doi.org/ 10.1021/acsomega.2c00651.

[8] Ghorbani, H., Wood, D.A., Choubineh, A., *et al*. 2020. Performance Comparison of Bubble Point Pressure from Oil PVT Data: Several Neurocomputing Techniques Compared. Exp. Comput. Multiph. Flow. 2: 225–246, https://doi.org/ 10.1007/s42757-019-0047-5.

[9] Ahmed, T. 2019. Chapter 2 - Reservoir-Fluid Properties. In Ahmed, T. (eds.), Reservoir Engineering Handbook, 5th ed. Gulf Professional Publishing. English. pp. 29–121.

[10] Abooali, D., Khamehchi, E. 2016. Toward Predictive Models for Estimation of Bubble Point Pressure and Formation Volume Factor of Crude Oil Using an Intelligent Approach. Braz. J. Chem. Eng. 33(4): 1083−1090, http://dx.doi.org/ 10.1590/0104-6632.20160334s20150374.

[11] Karimnezhad, M., Heidarian, M., Kamari, M., Jalalifar, H. 2014. A new empirical correlation for estimating bubble point oil formation volume factor. J. Nat. Gas Sci. Eng. 18: 329−335, https://doi.org/10.1016/j.jngse.2014.03.010.

[12] Larestani, A., Hemmati-Sarapardeh, A., Naseri, A. 2022. Experimental measurement and compositional modeling of bubble point pressure in crude oil systems: Soft computing approaches, correlations, and equations of state. J. Petro. Sci. Eng. 212: 110271, https://doi.org/10.1016/j.petrol.2022.110271.

[13] Elkatatny, S., Mahmoud, M. 2018. Development of a New Correlation for Bubble Point Pressure in Oil Reservoirs Using Artificial Intelligent Technique. Arab. J. Sci. Eng. 43: 2491−2500, https://doi.org/ 10.1007/s13369-017-2589-9.

[14] Mansour, E.M. 2020. Equation of State. Intech Open, http://dx.doi.org/10.5772/intechopen.89919.

[15] Neumann, T., Span, R. 2021. The Advantages of Equations of State in Form of the Helmholtz Energy for the Design of CCS-Relevant Processes. Energy Proc. 21, https://doi.org/10.46855/energy-proceedings-9357.

[16] Mansoori, G.A. 1986. Mixing Rules for Cubic Equations of State. Equ. State. 15: 314−330, http://dx.doi.org/10.1021/bk-1986-0300.

[17] Peng, D.-Y., Robinson, D.B. 1976. A New Two Constant Equation of State. Ind. Chemist. Eng. Fund. 15: 59−64, https://doi.org/10.1021/i160057a011.

[18] Alfradique, M.F., Castier, M. 2007. Calculation of Phase Equilibrium of Natural Gases with Peng Robinson and PC-SAFT Equations of State. J. Oil Gas Sci. Technol. 62(5): 707−714, http://dx.doi.org/ 10.2516/ogst:2007050.

[19] Valderrama, J. 2003. The State of the Cubic Equations of State. Ind. Eng. Chemist. Res. 42(8): 1603−1613, http://dx.doi.org/10.1021/ie020447b.

[20] Gross, J., Sadowski, G. 2001. Perturbed-Chain SAFT: An Equation of State Based on a Perturbation Theory for Chain Molecules. Ind. Chem. Res. 40(4): 1244−1260, http://dx.doi.org/ 10.1021/ie0003887.

[21] Fitzpatrick, D. 2018. Chapter 8 - Convergence Problems and Error Messages. In Fitzpatrick, D. (eds.), Analog Design and Simulation Using OrCAD Capture and Pspice, 2nd ed. Newnes. English. pp. 131−140.

[22] Nasir, Q., Sabil, K.M., Nasrifar, K. 2014. Measurement and Phase Behavior Modeling (Dew point and Bubble point) of CO_2 Rich Gas Mixture. J. Appl. Sci. 14(10): 1061−1066, http://dx.doi.org/10.3923/jas.2014.1061.1066.

[23] Hosein, R., Mayrhoo, R., McCain, W.D. Jr. 2014. Determination and Validation of Saturation Pressure of Hydrocarbon Systems using extended Y-functions. J. Pet. Sci. Eng. 124: 105−113, https://doi.org/10.1016/j.petrol.2014.10.022.

[24] Michelsen, M.L. 1985. Saturation point calculations. Fluid Phase Equilibr. 23(2−3): 181−192, https://doi.org/10.1016/0378-3812(85)90005-6.
[25] Medeiros, F.d.A.M., Stenby, E.H., Yan, W. 2021. Saturation Point and Phase Envelope Calculation for Reactive Systems Based on the RAND Formulation. Authorea. https//:doi.org/10.22541/ au.162076126.68762485/v1.
[26] Föll, F., Hitz, T., Müller, C. *et al*. 2019. On the use of tabulated equations of state for multi-phase simulations in the homogeneous equilibrium limit. Shock Waves. 29: 769−793, https://doi.org/ 10.1007/ s00193-019-00896-1.
[27] Ahmed, T., Nathan, M.D. 2010. A Practical Approach for Calculating EOS Coefficients SPE Russ. Oil Gas Conf. Exhibition.
[28] Coats, K.H., Smart, G.T. 1986. Application of a Regression-Based Equation of State PVT program to Laboratory Data. SPE Res. Eng. 1(03): 277−299, https://doi.org/10.2118/11197-PA.
[29] Whitson, C.H., Brule, M.R. 2000. Monograph, 20th ed. SPE. Richardson. pp. 1−233.
[30] Soreide, I. 1989. Improved Phase Behavior Predictions of Petroleum Reservoir Fluids from Cubic Equation of State [Dissertation]. Norwegian Institute of Technology. Norway.
[31] Ukwu, A.K. 2016. Performance Evaluation of Equation of State in Reservoir Fluid Modeling [Thesis]. University of Port Harcourt. Nigeria.
[32] Ashour, I., Al-Rawahi, N., Fatemi, A., Vakili-Nezhaad, G. 2011. Applications of Equations of State in the Oil and Gas Industry. Intechopen. https://doi.org/10.5772/23668.